

RESEARCH ARTICLE

Microstrip antenna with high self-interference cancellation using phase reconfigurable feeding network for in-band full duplex communication

Girdhari Chaudhary  | Junhyung Jeong  |
Yongchae Jeong | Woonchul Ham

Division of Electronic and Information Engineering, IT Convergence Research Center, Chonbuk National University, Jeonju, Republic of Korea

Correspondence

Yongchae Jeong and Woonchul Ham, Division of Electronic and Information Engineering, IT Convergence Research Center, Chonbuk National University, Jeonju, Republic of Korea.

Email: ycjeong@jbnu.ac.kr (Y. J.) and wcham@jbnu.ac.kr (W. H.)

Funding information

Basic Research Program through the NRF of Korea funded by the Ministry of Education, Grant/Award Number: 2019R1A6A1A09031717; Basic Science Research Program through the NRF of Korea funded by Ministry of Education, Science and Technology, Grant/Award Number: 2016R1D1A1B03931400; Korean Research Fellowship Program through the National Research Foundation (NRF) of Korea funded by the Ministry of Science and ICT, Grant/Award Number: 2016H1D3A1938065

Abstract

This article presents a bistatic microstrip circular patch antenna with high self-interference cancellation (SIC) through phase reconfigurable differential feeding network. The proposed microstrip antenna consists of closely spaced transmitter and receiver patches having orthogonal polarization with respect to each other. To achieve high SIC, the phase reconfigurable of feeding network can assist in tracking the phase offsets of self-interference signal caused by fabrication error or scattering nearby objects. From the experiment, the proposed antenna provided higher than 75 dB (65 dB) SIC bandwidth for 36 MHz (50 MHz) at the center frequency of 2.50 GHz. The proposed antenna is a good candidate for in-band full duplex communication system because of its simple design.

KEYWORDS

antenna self-interference cancellation (SIC), in-band full duplex (IBFD), microstrip antenna, passive SIC, phase reconfigurable feeding network

1 | INTRODUCTION

In-band full duplex (IBFD) system is one of the candidates for the next-generation 5G communication system because of its ability to enhance double spectral efficiency and data throughputs.¹ Its success depends on self-interference cancellation (SIC) capability to avoid signal to noise ratio degradation at the receiver side caused by transmitting strong self-interference (SI) signal. To prevent the saturation of receiver due to strong SI signal in the IBFD system, a SIC higher than 60 dB is essential at the antenna stage or RF analog cancellation stage.¹ Therefore, the antenna stage SIC can restrain receiver building blocks from saturation and relax the cancellations at another stage without complex cancellation circuitry.

To realize the IBFD operation with the required large amount of SIC, monostatic microstrip antennas using differential feeding, single tap and double tap RF-SIC circuits based on signal inversion techniques, were used.² Similarly, bistatic IBFD antennas (separate TX and RX antenna) were demonstrated using spatial duplexing, null placement, polarization diversity, differential feeding network and near field and feed-forward cancellation.³⁻⁷ The separate TX and RX antenna pair with orthogonal polarization and auxiliary port having reconfigurable reflective termination were presented in References 3,4. The reconfigurable reflective termination on auxiliary port reflects the coupled replica of leakage signal to cancel the SIC at RX port. Similarly, spatial filter based bistatic IBFD antenna was presented in Reference 5. Similarly, closely spaced bistatic patch antenna with satisfactory isolation between TX and RX port was realized in Reference 6, by using three interdigital lines that excited an orthogonal polarization mode on the adjacent patch. However, these techniques can provide SIC less than 40 dB, which is not enough for IBFD system.⁴⁻⁶ The asymmetrical coplanar strip (ACPS) wall was used to suppress the mutual coupling of the closely spaced bistatic IBFD antenna in Reference 8. The ACPS wall was inserted vertically between TX and RX antenna pair for canceling the direct coupling between two antennas. Electromagnetic band gap (EBG)

was used to increase the isolation between TX and RX antenna pair in Reference 9. A wideband dual-polarized bistatic IBFD antenna by employing two quad-ridge horns fed by ridge waveguide ortho-mode transducer was demonstrated in Reference 10. To improve the isolation between TX and RX ports, the high impedance surfaces (HIS) such as bed of nails (BONs) and metasurface were employed to reduce the coupling between TX and RX antennas. However, these works did not have a robust and resilient potential to tackle phase offsets of SI caused by fabrication error or scatters nearby objects.

In this study, microstrip antenna with high SIC is demonstrated in the bistatic configuration using phase reconfigurable feeding network. The proposed SIC technique has the potential to adjust phase offsets of the SI signal caused by fabrication error or scattering of nearby objects. As a result, high SIC is achievable in a robust environment without complex circuitry.

2 | MICROSTRIP ANTENNA WITH PHASE RECONFIGURABLE FEEDING NETWORK

Figure 1 shows a block diagram of the proposed IBFD antenna with phase reconfigurable feeding network. The proposed structure consists of closely spaced TX and RX circular patch radiating elements, which are in orthogonal polarization with respect to each other. The TX radiating patch is excited with phase reconfigurable differential feeding network whereas RX patch is excited with a single-ended co-axial

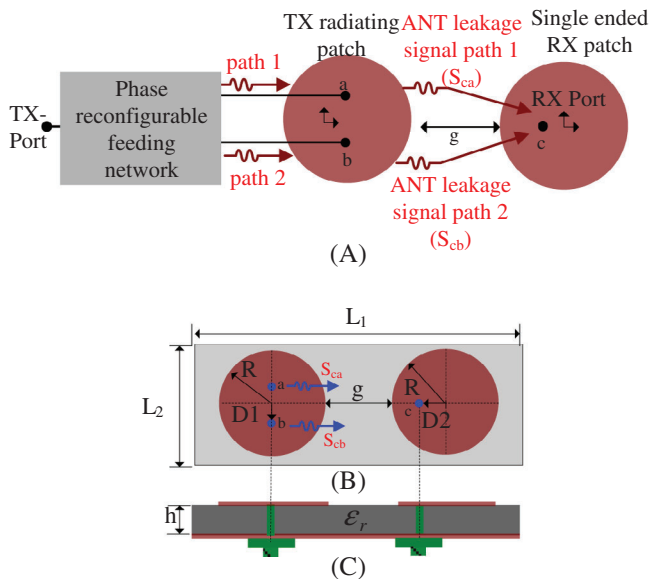


FIGURE 1 Proposed structure of antenna with phase reconfigurable feeding network for high SIC: A, block diagram of overall antenna; B, top view of closely spaced orthogonal polarized antenna; and C, side view. Physical dimensions: $L_1 = 120.4$, $L_2 = 69.2$, $R = 16.6$, $g = 10$, $D_1 = 4.3$, $D_2 = 5.3$, $h = 1.2$ (unit: millimeter) [Color figure can be viewed at wileyonlinelibrary.com]

feeding network. The proposed phase reconfigurable feeding network consists of a power dividing circuit and voltage-controlled varactor diodes for achieving flat phase characteristics. The SIC based on phase reconfigurable feeding network can be described by simple signal flow analysis as follows. Assuming input signal (S_i) at TX port is expressed as (1):

$$S_i(t, f) = A_i m_i(t) e^{-j(2\pi f t + \theta_i)}, \quad (1)$$

where $m_i(t)$ represents the unit RF signal having amplitude A_i , frequency f , and phase θ_i . The input RF signal is divided into two feeding output signals having equal magnitude and out-of-phase. These signals couple with leakage signal generated by the TX radiating element and are transferred to RX port as follows:

$$S_{\text{leakage}}^{\text{TX-RX}}(t, f) = \frac{A_i m_i(t)}{\sqrt{2}} \left\{ A_{1F} A_{1A} e^{-j(2\pi f t + \theta_i + \theta_{1F} + \theta_{1A})} - A_{2F} A_{2A} e^{-j(2\pi f t + \theta_i + \theta_{2F} + \theta_{2A})} \right\}, \quad (2)$$

where A_{iF} , θ_{iF} , A_{iA} , and θ_{iA} are amplitude and phase of feeding network output signals and antenna leakage signals, respectively.

As demonstrated in (2), the SIC depends on the amplitude and phase imbalances of feeding network output signals and antenna leakage signals. Assuming magnitude and phase imbalances of lossless feeding network as Δ_F and $\Delta\theta_F$, respectively, the TX-to-RX SIC can be derived as (3):

$$|S_{\text{SIC}}^{\text{TX-RX}}| = \frac{1}{\sqrt{2}} \sqrt{1 + \Delta_A^2 \Delta_F^2 - 2\Delta_F \Delta_A \cos(\Delta\theta_F + \Delta\theta_A)}, \quad (3)$$

where Δ_A and $\Delta\theta_A$ are magnitude and phase imbalances of leakage signal, respectively.

2.1 | Case 1: Constant amplitude and phase: $\Delta_A = 1$ and $\Delta\theta_A = 0^\circ$

When magnitude and phase of leakage signals through paths 1 and 2 are the same in overall frequency bandwidth, the TX-to-RX SIC fully depends on the performances of the feeding network. In such a case, infinite SIC can be achieved over the wideband if $\Delta_F = 0$ and $\Delta\theta_F = 0^\circ$. To investigate the effects of Δ_F and $\Delta\theta_F$, Figure 2 shows the calculated SIC of the proposed antenna by varying these parameters. As demonstrated in the figure, a TX-to-RX SIC higher than 70 dB can be achieved if feeding network magnitude and phase imbalances are within ± 0.1 dB and $\pm 1.5^\circ$, respectively.

2.2 | Case 2: Frequency-dependent variation of Δ_A and $\Delta\theta_A$

The magnitude and phase imbalances of antenna leakage signal change due to fabrication error or scatterings of objects. Therefore, the frequency-dependent values of Δ_A and $\Delta\theta_A$ can limit the TX-to-RX SIC within operating frequency bandwidth. To investigate these effects, the Δ_A and

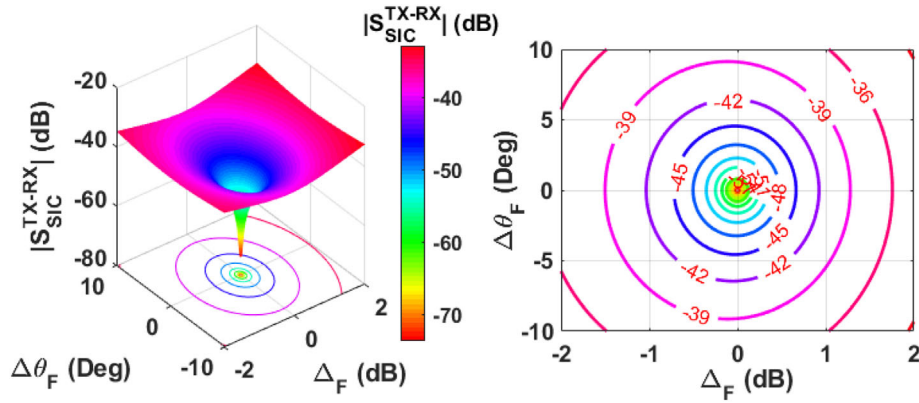


FIGURE 2 Calculated TX-to-RX SIC by varying magnitude and phase imbalances of feeding network with $\Delta_A = 1$ and $\Delta\theta_A = 0^\circ$ over all the frequencies [Color figure can be viewed at wileyonlinelibrary.com]

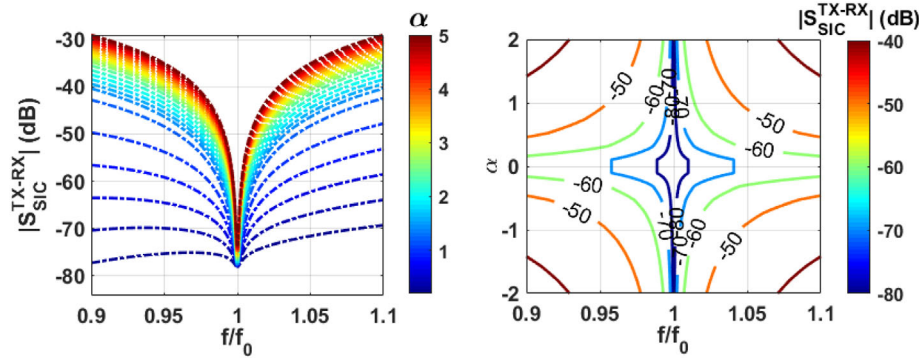


FIGURE 3 Calculated TX-to-RX SIC by varying Δ_A and $\Delta\theta_A$ monotonically according to the frequency with $\Delta_F = 0$ dB and $\Delta\theta_F = 1^\circ$ [Color figure can be viewed at wileyonlinelibrary.com]

$\Delta\theta_A$ were assumed to have monotonic variation with respect to frequency (f) as follows:

$$\Delta_A = 1 + \alpha(f - f_0/f_0) \quad (4a)$$

$$\Delta\theta_A = \beta(f - f_0/f_0) \quad (4b)$$

where f_0 , α , and β are center frequency, magnitude slop, and phase slope with respect to f , respectively.

Figure 3 shows the calculated TX-to-RX SIC by varying Δ_A and $\Delta\theta_F$ monotonically with respect to frequency. To achieve high SIC under these conditions, it is necessary to adjust the phase of the feeding network output signals for tracking the leakage signal. As demonstrated in Figure 3, a high SIC can be achieved within limited bandwidth if phase reconfigurable feeding network is applied. Also, the phase reconfigurable feeding network assist in achieving high SIC even though phase offsets change due to fabrication error or scatters nearby objects.

3 | SIMULATION AND MEASUREMENT RESULTS

To achieve the SIC under the magnitude and phase imbalance variations, the phase reconfigurable feeding network

was designed and fabricated using 3-dB hybrids and varactor diodes as shown in Figure 4. In the proposed feeding network, the coupled and through ports of one 3-dB hybrid were terminated with transmission lines (Z_0 , θ_0) and varactor diodes (C_v), whereas those of other hybrids are terminated with short-circuited transmission lines (Z_1 , θ_1) for achieving flat phase characteristics.¹¹ The feeding network was fabricated using substrate RT/Duroid 5880 ($\epsilon_r = 2.2$ and $h = 0.787$ mm) with circuit parameters $Z_1 = 40 \Omega$, $\theta_1 = 65^\circ$, $Z_0 = 50 \Omega$, and $\theta_0 = 35^\circ$. Similarly, 3-dB 90° hybrids S03A2500N1 from ANAREN were used in this work because of their wideband characteristics. The varactor SMV-1231 from Skyworks with parasitic components $L_s = 0.7689$ nH, $R_s = 1.5 \Omega$, and $C_p = 0.27$ pF is used. The C_v is varied from 0.42 pF to 4.17 pF at $f_0 = 2.5$ GHz when the bias voltage applied from 18 to 0 V.

Figure 5 shows the simulated and measured amplitude and phase balance responses of the feeding network output signals. The phase balance of the proposed feeding output signals was reconfigured from 160° to 195° with a maximum phase error of $\pm 1.2^\circ$ within the bandwidth of 200 MHz at $f_0 = 2.50$ GHz. Similarly, amplitude balances are varied from 0.1 to -0.23 dB within the bandwidth of 200 MHz at $f_0 = 2.50$ GHz.

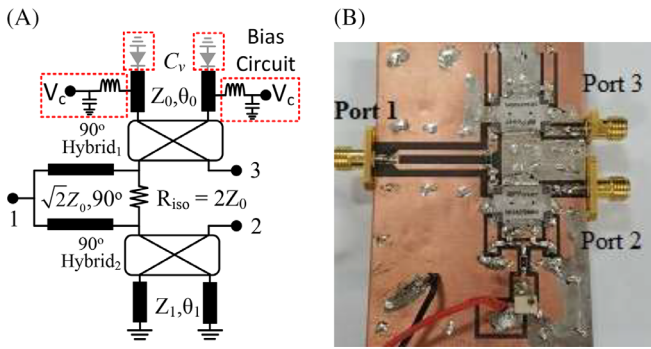


FIGURE 4 Structure of phase reconfigurable feeding network: A, circuit diagram; and B, fabricated photograph [Color figure can be viewed at wileyonlinelibrary.com]

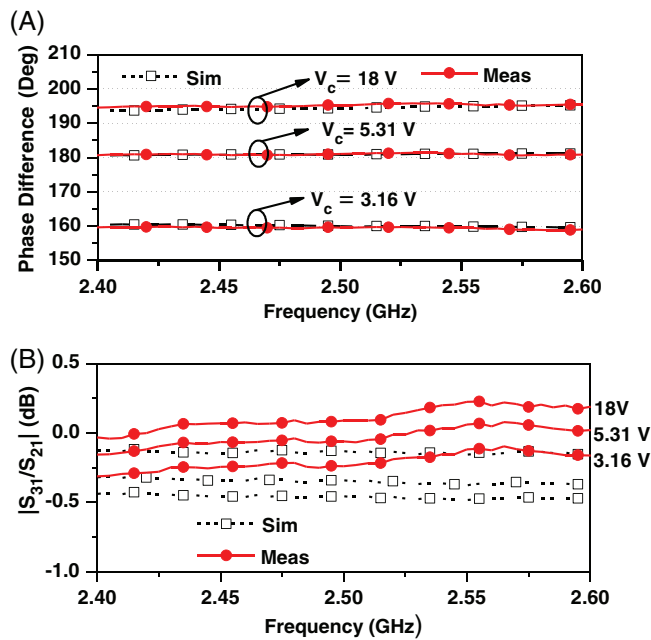


FIGURE 5 Simulated and measured results of proposed phase reconfigurable feeding network: A, phase; and B, magnitude balances [Color figure can be viewed at wileyonlinelibrary.com]

The IBFD antenna was designed and fabricated at $f_0 = 2.5$ GHz using FR-4 substrate ($\epsilon_r = 4.4$, $h = 1.2$ mm, $\tan \delta = 0.02$). The TX and RX patches are placed on same surface of the ground plane as shown in Figure 1. The TX antenna is excited with reconfigurable phase feeding network which have 180° phase shift. The physical dimensions of the antenna are shown in Figure 1. The proposed antenna is simulated by using ANSYS HFSS.

Figure 6 shows the simulated TX-to-RX leakages through path 1 (S_{ca}) and path 2 (S_{cb}) according to separation distance (g) between TX and RX patches. As seen from figure, the magnitude of TX-to-RX leakage is decreased if g increases. In addition, the amplitude (Δ_A) and phase imbalances ($\Delta\phi_A$) are also affected. For high SIC, the variations of Δ_A and $\Delta\phi_A$ should be as small as possible. Similarly,

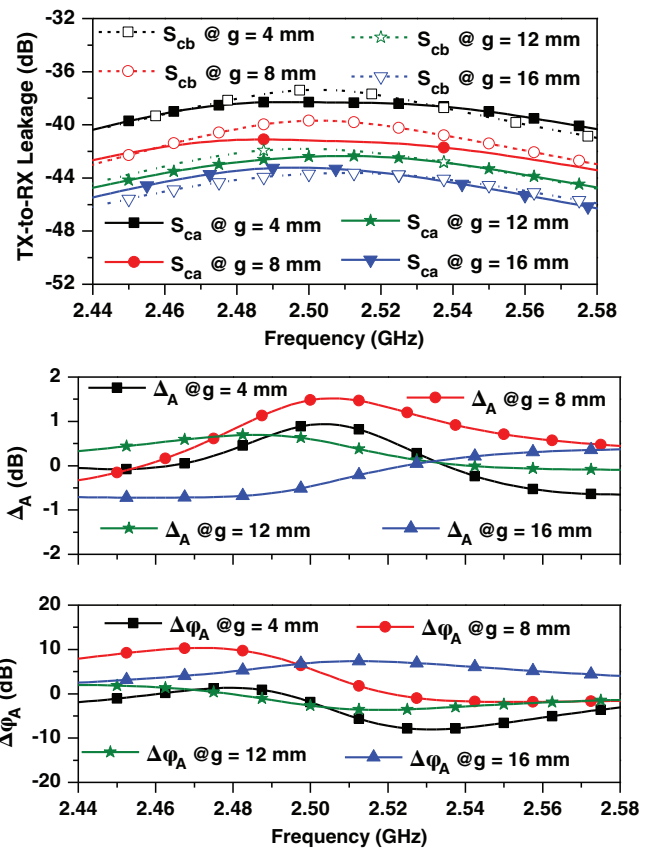


FIGURE 6 Simulated TX-to-RX antenna leakage signals according to separation between TX to RX patches [Color figure can be viewed at wileyonlinelibrary.com]

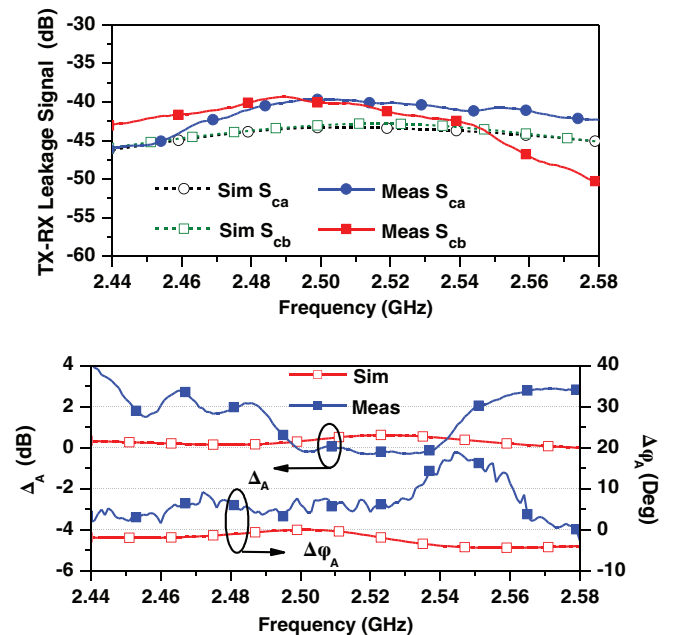


FIGURE 7 Simulated and measured TX-to-RX antenna leakage signals [Color figure can be viewed at wileyonlinelibrary.com]

Figure 7 shows the simulated and measured S_{ca} and S_{cb} between TX and RX antennas. The measured S_{ca} and S_{cb} have almost same magnitude of -40 dB, which is due to

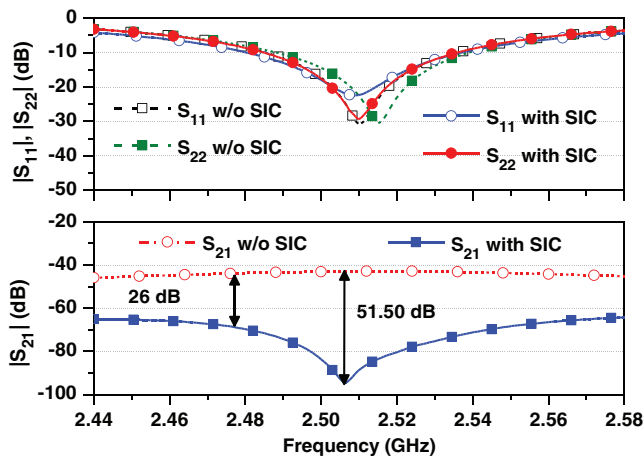


FIGURE 8 Simulated $|S_{11}|$, $|S_{22}|$, and $|S_{21}|$ with and without SIC circuit [Color figure can be viewed at [wileyonlinelibrary.com](#)]

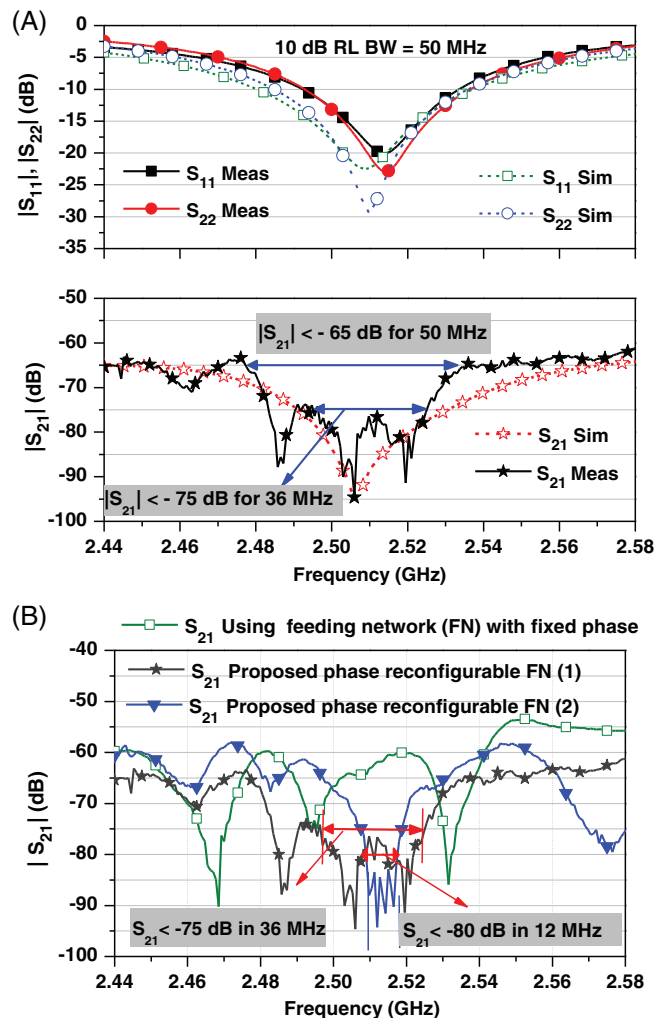


FIGURE 9 Experimental results for implemented IBFD antenna with phase reconfigurable feeding network: A, proposed antenna with reconfigurable feeding network; and B, magnitude of $|S_{21}|$ using proposed phase reconfigurable feeding network and conventional feeding network with fixed phase (such as ring hybrid) [Color figure can be viewed at [wileyonlinelibrary.com](#)]

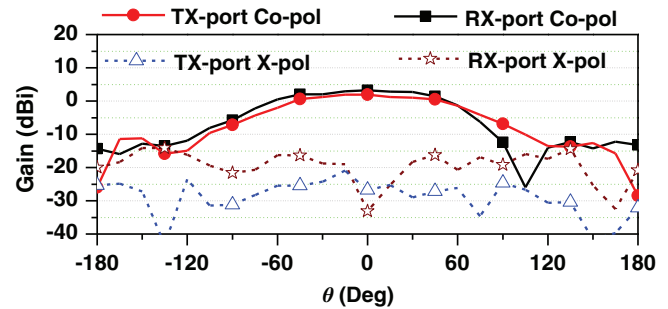


FIGURE 10 Measured antenna gains and cross-polarization level [Color figure can be viewed at [wileyonlinelibrary.com](#)]

combination of orthogonal polarization and spatial isolation. The measured Δ_A and $\Delta\varphi_A$ of leakage signal between TX and RX antenna are given as 0.96 ± 0.1 dB and $4.2 \pm 2^\circ$ over 100 MHz at $f_0 = 2.50$ GHz, respectively. The high Δ_A and $\Delta\varphi_A$ of antenna leakage signals are due to fabrication error, which will prevent a perfect elimination of the self-interference signals. Similarly, Figure 8 shows the simulated the S -parameters of the proposed antenna with and without SIC circuit. From Figure 8, we conclude that the proposed phase reconfigurable feeding network can improve SIC between TX to RX ports by 50.51 dB at $f_0 = 2.51$ GHz and 26 dB for 2.483 to 2.536 GHz.

Figure 9 shows the simulated and measured input and output return losses (S_{11} and S_{22}) and TX-to-RX SIC (S_{21}) results for the overall implemented circuit. The measurement was taken in a laboratory environment. The measured 10 dB return loss bandwidth was 50 MHz (2.49–2.54 GHz). Similarly, the measured TX-to-RX SIC showed that the isolation was higher than 75 dB in 36 MHz bandwidth and 65 dB in 50 MHz bandwidth as compared to 60 dB for conventional feeding network with fixed phase (such as ring hybrid) case. The high TX-to-RX isolation is achieved by combination of orthogonal polarization, spatial isolation, and SIC through phase reconfigurable feeding network. The orthogonal polarization and spatial techniques provide approximately 40 dB TX-to-RX isolation whereas SIC through phase reconfigurable feeding network provides approximately 35 dB. In addition, the proposed IBFD antenna with phase reconfigurable feeding network provides 15 dB higher SIC than the fixed feeding network.

Figure 10 shows the measured gain and cross-polarization of the implemented antenna. The measured TX and RX antenna peak gains are 2.9 and 3.8 dBi, respectively. The TX antenna gain is slightly lower than RX antenna gain because of insertion loss of phase reconfigurable feeding network. Similarly, the measured cross-polarization levels are 20 dB down with respect to the co-polarization level. The performances comparison of the proposed bistatic IBFD antenna with state-of-arts was as depicted in Table 1. As shown from the table, the proposed antenna provided highest SIC as compared to state-of-arts. Although stat-of-arts

TABLE 1 Performance comparison of proposed IBFD antenna with state-of-arts

	f_0 (GHz)	SIC/BW (dB/MHz)	ANT separation	ANT size	SIC techniques
3	4.60	50/300	$0.08\lambda_0$	$0.921\lambda_0 \times 0.760\lambda_0$	Polarization diversity
4	2.50	40/200	$0.10\lambda_0$	$1.081\lambda_0 \times 0.750\lambda_0$	Polarization diversity
5	0.85	25/10	$0.31\lambda_0$	$0.311\lambda_0 \times 0.155\lambda_0$	Spatial duplexing
6	5.80	20/270	$0.07\lambda_0$	$0.881\lambda_0 \times 0.580\lambda_0$	Interdigital lines
7	2.50	60/110	$0.08\lambda_0$	$1.066\lambda_0 \times 0.6\lambda_0$	DFN
8	5.80	35/80	$0.03\lambda_0$	$0.862\lambda_0 \times 0.58\lambda_0$	ACPS wall
10	10	70/2000	$6.66\lambda_0$	$12.66\lambda_0 \times 4.33\lambda_0$	QRH with HIS
12	2.45	60/150	$0.09\lambda_0$	$1.192\lambda_0 \times 0.469\lambda_0$	PRC
This work	2.50	75/36	$0.08\lambda_0$	$1.038\lambda_0 \times 0.585\lambda_0$	PRFN

Abbreviations: ACPS, asymmetrical coplanar strip; DFN, differential feeding network; HIS, high impedance surface; IBFD, in-band full duplex; PRC, phase reconfigurable coupler; PRFN, phase reconfigurable feeding network; QRH, quad-ridge horn; SIC, self-interference cancellation.

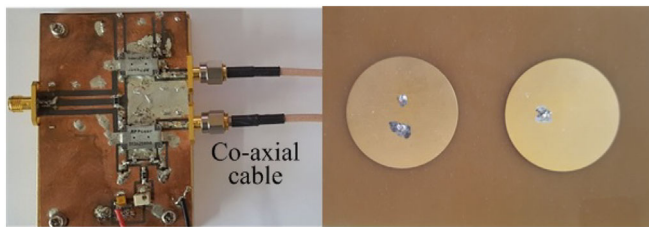


FIGURE 11 Photograph of fabricated antenna including phase reconfigurable feeding network [Color figure can be viewed at wileyonlinelibrary.com]

provide wide SIC bandwidth, the SIC is limited to 50 dB.³⁻⁶ The photograph of fabricated antenna is shown in Figure 11. The overall size of antenna is $1.038\lambda_0 \times 0.585\lambda_0$, where λ_0 is a wavelength at the center frequency.

4 | CONCLUSION

This study proposed a bistatic antenna with high SIC for a full duplex system using phase reconfigurable feeding network. The analytical design equations were derived to assist in the design of the antenna under magnitude and phase imbalance variations due to fabrication error or scatterings nearby objects. The proposed antenna can provide higher TX-to-RX self-interference cancellation as compared to the fixed feeding network. The easy implementation and good performances show that the proposed antenna is suitable for achieving high self-interference cancellation under robust environments.

ACKNOWLEDGMENT

This research was supported by the Korean Research Fellowship Program through the National Research Foundation (NRF) of Korea funded by the Ministry of Science and ICT (2016H1D3A1938065) and in part by the Basic Science Research Program through the NRF of Korea funded by Ministry of Education, Science and Technology

(2016R1D1A1B03931400) and in part by the Basic Research Program through the NRF of Korea funded by the Ministry of Education (2019R1A6A1A09031717).

ORCID

Girdhari Chaudhary  <https://orcid.org/0000-0003-2060-9860>

Junhyung Jeong  <https://orcid.org/0000-0003-2383-1635>

REFERENCES

- [1] Hong S, Brand J, Choi J, et al. Applications of self-interference cancellation in 5G and beyond. *IEEE Commun Mag.* 2014;14:114-121.
- [2] Nawaz H, Gurbuz O, Tekin I. 2.4 GHz dual polarized monostatic antenna with simple two-tap RF self-interference cancellation (RF-SIC) circuitry. *IET Electron Lett.* 2019;55:299-300.
- [3] Dinc T, Krishnaswamy H. A T/R antenna pair with polarization based reconfigurable wideband self-interference cancellation for simultaneous transmit and receive. Paper presented at: IEEE MTT-S International Microwave Symposium Digest; 2015:1-4.
- [4] Wang X, Che W, Yang W, Feng W, Gu L. Self-interference cancellation antenna using auxiliary port reflection for full-duplex application. *IEEE Antennas Wirel Compon Lett.* 2017;16:2873-2876.
- [5] Alrabadi ON, Tatomiurescur A, Knudsen MB, Pelosi M, Pedersen GF. Breaking the transmitter-receiver isolation barrier in mobile handsets with spatial duplexing. *IEEE Trans Antenna Propag.* 2013;61:2241-2251.
- [6] Qi H, Yin X, Liu L, Rong Y, Qian H. Improving isolation between closely spaced patch antennas using interdigital lines. *IEEE Antennas Wirel Propag Lett.* 2016;15:286-289.
- [7] Chaudhary G, Jeong J, Jeong Y. Differential fed antenna with high self-interference cancellation for in-band full duplex communication system. *IEEE Access.* 2019;7:45340-45348.
- [8] Qi H, Liu L, Yin X, Zhao H, Kulesza WJ. Mutual coupling suppression between two closely spaced microstrip antennas with an asymmetrical coplanar strip wall. *IEEE Antenna Propag Lett.* 2016;15:191-194.
- [9] Sievenpiper D, Zhang L, Broas RFJ, Alexopolus NG, Yablonovitch E. High impedance electromagnetic surfaces with a

- forbidden frequency band. *IEEE Trans Microw Theory Tech.* 1999;47:2059-2074.
- [10] Prasananakumar PV, Elmansouri MA, Filipovic DE. Wideband decoupling techniques for dual-polarized bi-static simultaneous transmit and receive antenna system. *IEEE Trans Antenna Propag.* 2017;65:4991-5001.
- [11] Chaudhary G, Jeong Y. Wideband tunable differential phase shifter with minimized in-band phase deviation error. *IEEE Microw Wirel Compon Lett.* 2019;29:468-470.
- [12] Khaledian S, Farzami F, Smida B, Erricolo D. Robust self-interference cancellation for microstrip antennas by means of phase reconfigurable coupler. *IEEE Trans Antennas Propag.* 2018;66:5574-5579.

How to cite this article: Chaudhary G, Jeong J, Jeong Y, Ham W. Microstrip antenna with high self-interference cancellation using phase reconfigurable feeding network for in-band full duplex communication. *Microw Opt Technol Lett.* 2020;62:919–925. <https://doi.org/10.1002/mop.32104>